The Canadian Mineralogist
Vol. 39, pp. 1081-1094 (2001)

COLLINSITE IN HYDROTHERMAL ASSEMBLAGES RELATED TO CARBONATITES IN THE KOVDOR COMPLEX, NORTHWESTERN RUSSIA

RUSLAN P. LIFEROVICH[§]

Institute of Geosciences, University of Oulu, PL-3000, FIN-90014 Oulu, Finland

YAKOV A. PAKHOMOVSKY, ALLA N. BOGDANOVA AND ELENA G. BALAGANSKAYA

Geological Institute, Kola Science Centre, Russian Academy of Sciences, 14 Fersmana Street, 184200-RU Apatity, Russia

KAUKO V.O. LAAJOKI AND SEPPO GEHÖR

Institute of Geosciences, University of Oulu, PL-3000, FIN-90014 Oulu, Finland

NIKITA V. CHUKANOV

Institute of Chemical Physics, Russian Academy of Sciences, Chernogolovka, Moscow Region, 142432, Russia

ABSTRACT

Several generations of collinsite were formed during the hydrothermal alteration of phoscorite and dolomite carbonatite in the Kovdor alkaline-ultramafic complex, northwestern Russia. The collinsite at this locality shows isomorphic substitution of Sr for Ca at the *A* crystallographic site, which is atypical both for this species and for the entire fairfieldite group. The Sr content reaches 0.74 atoms per formula unit and shows an inverse correlation with Ca. Sr is found to account for no more than 37% of the total occupancy of the *A* site, a proportion that fits the Lewis acidity of interstitial cations, a value of 0.25 valence units (assuming a disordered distribution of Sr), which in turn matches the Lewis basicity of the structural unit in collinsite, the chain [$Mg(PO_4)_2(H_2O)_2$]. The collinsite-bearing assemblages were formed by juvenile hydrothermal solutions derived from phoscorites and carbonatites that had been cooling in a tectonically active environment. Textural evidence and strontium isotopic characteristics show that the assemblages were superimposed upon the host rocks after the cataclasis of the dolomite carbonatite and selective leaching of its primary minerals. The Sr isotopic composition of collinsite and the associated hydrothermal phosphates shows no contribution from any crustal component. Being confined to faults, the orthomagmatic hydrothermal solutions migrated upward and were not mixed with groundwater or crustal fluids in tectonic channels prior to deposition of the collinsite-bearing assemblages. The active fluid–rock interaction below 270°C under wide variations in pH–Eh parameters, $f(O_2)$, $f(S_2)$, and relatively low $f(CO_2)$ did not homogenize the isotopic composition of Sr between the solutions and the affected carbonate rock.

Keywords: collinsite, strontian, hydrothermal, juvenile, phosphate, electron-microprobe analysis, carbonatite, Kovdor Complex, Russia.

SOMMAIRE

Plusieurs générations de collinsite ont été déposées lors de l’altération hydrothermale de la phoscorite et de la carbonatite à dolomite du complexe alcalin et ultrabasique de Kovdor, dans le nord-ouest de la Russie. La collinsite de cet endroit fait preuve d’une substitution du Sr pour le Ca dans le site *A* de la structure, ce qui n’est pas typique de cette espèce ou des membres du groupe de la fairfieldite en général. La teneur en Sr atteint 0.74 atomes par unité formulaire et montre une corrélation inverse avec la teneur en Ca. Le Sr atteint donc une teneur maximale de 37% du site *A*, une proportion qui concorde avec la prédiction faite à partir de l’équivalence de l’acidité de Lewis des cations interstitiels, 0.25 unités de valence (en supposant une distribution désordonnée du Sr), et de la basicité de Lewis de la chaîne [$Mg(PO_4)_2(H_2O)_2$], le module structural de la collinsite. Les assemblages à collinsite se sont formés à partir de solutions hydrothermales juvéniles dérivées des phoscorites et des carbonatites au cours de leur refroidissement dans un milieu tectoniquement actif. D’après l’évidence texturale et les caractéristiques des isotopes de strontium, les assemblages ont été imposés aux roches-hôtes après la cataclase de la carbonatite à dolomite et le lessivage sélectif de ses minéraux primaires. La composition isotopique du Sr dans la collinsite et les phosphates hydrothermaux associés

---

[§] *E-mail address*: life@cc.oulu.fi. *Permanent address*: Geological Institute, Kola Science Centre, Russian Academy of Sciences, 14 Fersmana Street, 184200-RU, Apatity, Russia. life@geoksc.apatity.ru

ne révèle aucun apport de la croûte. Confinée aux plans de failles, la phase fluide orthomagmatique a monté sans se mélanger aux nappes d'eau souterraines ou aux fluides d'origine crustale dans les chenaux d'origine tectonique avant de déposer les assemblages à collinsite. L'interaction entre roche et phase fluide aqueuse à une température inférieure à 270°C en présence de fluctuations importantes en conditions de pH–Eh, $f(O_2)$, $f(S_2)$, et à $f(CO_2)$ relativement faible, n'a pas permis une homogénéisation des isotopes de Sr entre les solutions et les roches carbonatées affectées.

(Traduit par la Rédaction)

Mots-clés: collinsite, strontifère, hydrothermal, juvénil, phosphate, données à la microsonde électronique, carbonatite, complexe de Kovdor, Russie.

INTRODUCTION

Hydrothermal activity commonly accompanies the waning stages of formation of highly evolved carbonatites and phoscorites. The composition of the hydrothermal assemblages depends more on the postmagmatic tectonic regime than on the composition of the magmas parental to the mineralizing fluid, which implies that in many instances, the late mineralization involves disequilibrium conditions. In particular, the carbonatites in Kovdor complex, Kola Alkaline Province, northwestern Russia, contain hydrothermal assemblages dominated by rare phosphates of magnesium, but do not contain *F*- and *REE* minerals that are typical of the late assemblages related to similar carbonatites elsewhere (*i.e.*, the Vuorijarvi, Seblyavr, Sokli and Palaborwa complexes). This peculiarity seems to be due to the openness of the hydrothermal system and to the intense alteration of the various primary minerals in phoscorites and carbonatites of the Kovdor complex.

We describe in this paper the occurrence of collinsite in hydrothermal mineral assemblages enclosed by altered phoscorites and carbonatites in the Kovdor alkaline-ultramafic complex, and report on the chemical composition of the collinsite and some features of its genesis. We thus shed light on the late stage of evolution of the mantle-derived melt–fluid system that entered the upper crust.

BACKGROUND INFORMATION

There is a paucity of data on minerals of the fairfieldite group, in general $A_2B[TO_4]_2 \cdot 2H_2O$, where A = Ca, B = Mg, Fe, Mn, Zn, Ni, or Co, and T = P, As, and in particular on the Ca–Mg–P member of this group, collinsite. The collinsite of the Kovdor complex was originally described in vuggy phoscorite and carbonatite by Rimskaya-Korsakova (1965), who found this mineral to be non-stoichiometric and enriched in Sr and Ba (3.51 wt.% SrO, 1.23% BaO). Kapustin (1980) suggested that these data, acquired by wet-chemical analysis, reflected contamination by impurities, and described Sr-free collinsite in the same massif. An X-ray-diffraction pattern similar to the ASTM 14–314 standard (currently marked as obsolete in the ASTM powder-diffraction file) was obtained for this sample of collinsite. Nevertheless, the strontian variety of collinsite (6.3 wt.% SrO) was again found in a hydrothermal assemblage with strontiowhitlockite by Britvin *et al.* (1991).

Kapustin (1980) mentioned that some etched samples of collinsite from the Kovdor complex are covered with products of alteration of the mineral. Upon preliminary examination, we found such material to be covered with tiny crystals of a late phosphate. A single qualitative estimate of the composition of this late phosphate suggests that it is messelite (Liferovich *et al.* 2000a).

Our study of hydrothermal assemblages in the carbonatites of the Kovdor complex has confirmed the presence of strontian collinsite. Moreover, we have found this variety to be predominant in the Kovdor complex. In some cases, the collinsite contains significantly more Sr than was originally described.

GEOLOGICAL SETTING

The Kovdor complex results from the multiphase emplacement of alkaline-ultramafic silicate rocks, phoscorites and carbonatites into Archean biotite gneisses (Kukharenko 1965). The general geology of the intrusion has been described in detail by Kogarko *et al.* (1995) and Verhulst *et al.* (2000), among others. The massif is predominantly composed (from the older core toward the younger periphery) of dunite, clinopyroxenite, jacupirangite and rocks of the ijolite–melteigite series. Between the core and the periphery, there are discontinuous zones of turjaite, melilitolite, clinopyroxene–olivine rock enriched with phlogopite, garnet – amphibole – monticellite rock, nepheline pyroxenite, and bodies of phoscorite and carbonatite.

The largest body of multistage carbonatite and phoscorite is a 0.8 × 1.3 km stock. It intruded clinopyroxenite and ijolite–melteigite at the intersection of N- and NE-trending faults 380 ± 4 Ma ago (Dunaev 1982, Bayanova *et al.* 1997). The geology, petrography and mineralogy of the stock were studied in great detail (Ternovoi 1977, Krasnova & Kopylova 1988, and references therein). The dominant calcite phoscorites and carbonatites give way to less abundant dolomite-bearing varieties, and the late dolomite carbonatite forms a linear system of mutually subparallel veins. This system formed mostly along the NE-trending fault, where steeply dipping fractures are filled by dolomite veins 0.1–3 m thick and 20–150 m long that have been traced down by drilling to a depth of almost 2 km (Khomyakov *et al*. 1982).

The available Sr and Nd isotope data show the phoscorites and carbonatites to be derived from the depleted mantle (Zaitsev & Bell 1995, Verhulst *et al.* 2000). The initial Sr isotope ratio of phoscorite and carbonatite ranges from 0.70320 to 0.70395. Apatite, calcite and dolomite from the same rocks show less variation: $(0.70330 < (^{87}Sr/^{86}Sr)_i < 0.70363$ (Zaitsev & Bell 1995, Verhulst *et al.* 2000). Some dolomite carbonatite has a whole-rock $(^{87}Sr/^{86}Sr)_i$ as high as 0.70470(10) (Landa *et al.* 1982).

Postmagmatic activity along faults occurred in the Kovdor phoscorite–carbonatite stock and was accompanied by local hydrothermal alteration in the enclosing rocks. Cataclasis in the NE-trending fault mostly affected the dolomite carbonatite veins that had been filled this fault at the late magmatic stage, whereas the N-trending fault intersected all the rock varieties. Some primary minerals in carbonatite and phoscorite (mostly pyrrhotite and, to a lesser extent, fluorapatite, forsterite and phlogopite), were subject to intense hydrothermal alteration and replacement by other minerals, whereas the rock-forming dolomite was not dissolved (Liferovich *et al.* 2000b). Ponomareva & Krasnova (1990) proposed that some hypothetical primary phosphate (probably newberyite) had also been dissolved in the dolomite veins, leaving cavities. Postmagmatic processes have formed numerous cracks, fissures and cavities in affected rocks and imparted a vuggy texture to the altered dolomite veins. It is in the vicinity of such vugs that the most intensive alteration of primary minerals took place along axial zones and endocontacts, where cracks and fissures are more abundant. The less affected intermediate zones commonly contain fresh aggregates of the primary fluorapatite and phlogopite. Intense cataclasis and alteration in the N-trending fault zone caused serpentinization of the phoscorites and formation of subvertical slickensides and cracks, commonly filled with late hydroxylapatite, dolomite and calcite.

DESCRIPTION OF COLLINSITE AND ITS OCCURRENCE

Two types of collinsite-bearing assemblages occur in the Kovdor massif: i) assemblages that line vugs and fissures in altered dolomite carbonatite confined to the NE-trending fault, and ii) assemblages in mineralized fissures in serpentine–magnetite cataclasite formed after phoscorites along the N-trending fault.

Several generations of collinsite appear sporadically in assemblages of the first type throughout the vuggy dolomite carbonatite studied, *e.g.* it is found down to 1900 m in the drill core. The collinsite in vugs and fissures is associated with late magnetite (soot-like masses replacing primary pyrrhotite), euhedral late sulfides (pyrite or pyrrhotite, hexagonal according to X-ray diffraction) and all the hydrated Fe- and Mg-phosphates known in the Kovdor.

Collinsite in assemblages of the second type occasionally occurs in small cracks filled with calcite and hydroxylapatite and enclosed by serpentine–magnetite cataclasite. The same rock was found to enclose a stockwork of mineralized fissures lined with collinsite and kovdorskite (Fig. 1) at a depth of 250–270 m from the surface; this zone was stripped and mined out in 1996. This occurrence contained an outstanding volume of rare hydrothermal phosphates. The stockwork was as thick as 3–5 m and was traced along the strike and dip directions for some tens of meters. Mineralized cavities up to 0.5 m^3 in size were confined to shear fractures, and the walls of vugs were lined with collinsite–kovdorskite druses, some of which provide evidence of multiple intramineralization adjustments (Figs. 1c–e). For example, collinsite and kovdorskite may show an alternation of clear zones with zones filled with magnetite and dolomite particles. The number of zones reaches 15, and a regular upward diminution in particle size was observed in each (Figs. 1d, e) in accordance with the principles of sedimentation in a liquid medium (Stokes's law). The kovdorskite druses are covered with a fine-grained kovdorskite and magnetite "regolith" in places, and some have been mechanically damaged *in situ* and even cut by slickensides (Fig. 1c).

At Kovdor, the collinsite occurs as lath-like fibers elongate along [100] and arranged in reniform masses with a serrate surface (Fig. 2a), although it may also form spherulites or clusters of bladed crystals (Fig. 2b). The habit of the collinsite is very similar to that of collinsite in the Yukon (Robinson *et al.* 1992). The prismatic crystals described previously in the Kovdor massif (Kapustin 1980) and at Milgun, Australia (Bridge & Pryce 1974) were not found in this study.

ANALYTICAL TECHNIQUES

The chemical composition of collinsite was determined by the wavelength-dispersion X-ray technique (WDS) with a Cameca MS–46 electron microprobe at the Kola Science Centre, Russia. The electron beam was defocused to 30 μm, and the samples were moved during the analysis so as to minimize decomposition of the mineral under the beam. The following were used as standards: synthetic $AlPO_4$ (P), apatite (Ca), forsterite (Mg), celestine (Sr), barite (Ba), synthetic $MnCO_3$ (Mn) and hematite (Fe). The raw data were ZAF-corrected. The H_2O content of a sample of ordinary collinsite and of the most Sr-rich sample was established by thermogravimetric analysis (courtesy of Dr. D.V. Makarov). Semi-quantitative energy-dispersion X-ray analyses (EDS) and evaluation of collinsite homogeneity in back-scattered electron images were carried out at the University of Oulu using a JEOL JSM–6400 scan-

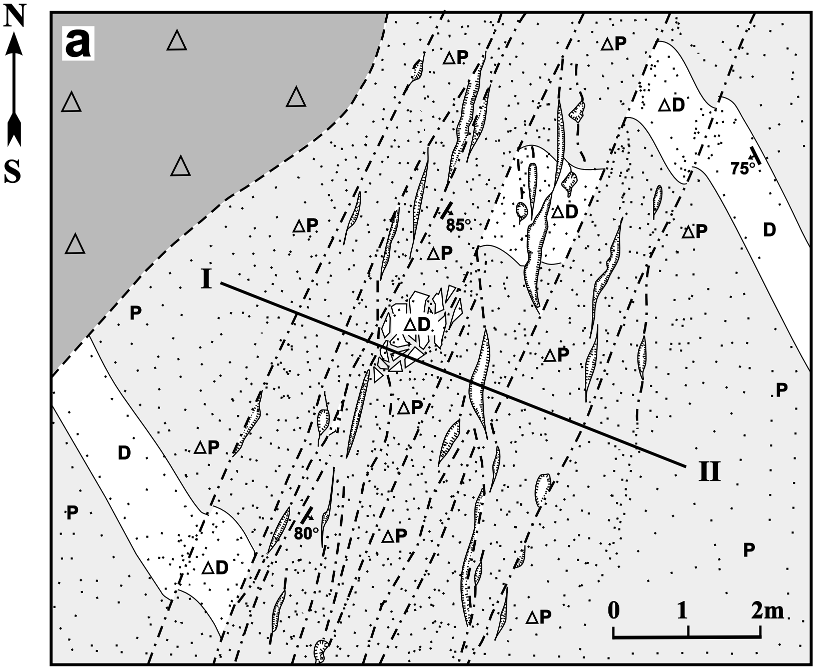

FIG. 1. Collinsite–kovdorskite stockwork in the N-trending fault-zone that cross-cuts the phoscorites and carbonatites. (a) Sketch map. (b) Geological section. (c) Druse of collinsite and kovdorskite lining a fissure. (d) Zoned crystal of kovdorskite crystal composed of zones contaminated by magnetite–dolomite particles (clasts) alternating with water-clear zones. (e) Contaminated zone in a kovdorskite crystal, showing an upward gradation in the size of the particles.

ning electron microscope. The powder infrared-absorption spectra were obtained with a Specord–75 spectrophotometer. A DRON–2 diffractometer (Cu*K*α radiation, SiO_2 monochromator, 30 kV, 40 mA) was employed to obtain X-ray-diffraction patterns of the several generations of collinsite with gradually increasing abundances of Sr.

Phosphate samples that had been hand-picked for Sr isotopic analyses were dissolved in a HNO_3–HCl mixture, and Rb and Sr were separated by conventional ion-exchange techniques, and their concentrations were determined by isotope dilution using single ^{87}Rb and ^{84}Sr spikes. Sr isotope ratios were measured using a MI–1201T mass spectrometer operated in double Re-filament mode and normalized to $^{86}Sr/^{88}Sr = 0.1194$ (Steiger & Jäger 1977). The NBS SRM–987 standard gave measured $^{87}Sr/^{86}Sr$ values of 0.71044 ± 0.0004 during the run period. The reproducibility of the $^{87}Sr/^{86}Sr$ values is quoted to be about 0.04% (2σ). To verify the results, an apatite sample with a known $^{87}Sr/^{86}Sr$ ratio was analyzed. Fluorapatite from the huge phlogopite – olivine – diopside pegmatite (the Kovdor phlogopite deposit) gave a $^{87}Sr/^{86}Sr$ value of 0.70340(14), which is in full accord with the value obtained by Landa *et al.* (1982) for a similar sample.

TABLE 1. REPRESENTATIVE COMPOSITIONS OF COLLINSITE FROM THE KOVDOR HYDROTHERMAL ASSEMBLAGES

	1	2	3	4	5	6	7	8	9	10
CaO	32.89	33.40	29.99	27.96	27.43	24.33	21.53	32.54	19.02	19.14
SrO	0.25	0.30	3.65	6.88	7.02	12.19	16.65	2.09	20.87	20.05
BaO	n.d.	n.d.	1.79	1.88	0.77	2.17	1.36	0.42	1.60	1.66
MgO	11.64	7.87	10.89	11.18	11.56	9.64	9.71	11.37	10.25	10.28
MnO	0.41	0.41	0.16	0.37	0.84	0.60	0.73	0.29	0.79	0.71
FeO	0.27	5.73	0.10	n.d.	0.42	1.30	0.58	0.90	0.13	0.10
P_2O_5	43.44	40.35	41.44	40.83	41.56	40.95	39.48	42.65	39.25	39.35
H_2O	11.07*	10.55§	10.28§	10.33§	10.40§	9.98§	9.76§	10.83§	8.92*	9.76§
total	99.97	98.61	98.30	99.43	100.0	101.16	99.80	101.09	100.83	101.05
Atoms per formula unit on the basis of Σ R^{2+} cations = 3										
Ca	1.98	2.03	1.88	1.74	1.70	1.57	1.42	1.93	1.24	1.26
Sr	0.01	0.01	0.12	0.23	0.23	0.42	0.59	0.07	0.74	0.71
Ba	-	-	0.04	0. 04	0.02	0.05	0.03	0.01	0.04	0.04
Mg	0.98	0.67	0.95	0.97	0.99	0.86	0.89	0.94	0.93	0.94
Mn	0.02	0.02	0.01	0.02	0.04	0.03	0.04	0.01	0.04	0.04
Fe	0.01	0.27	-	-	0.02	0.07	0.03	0.04	0.01	0.01
P	2.07	1.94	2.05	2.0	2.03	2.08	2.05	2.0	2.03	2.05
H_2O	2.08	2	2	2	2	2	2	2	1.82	2

* H_2O determined by loss on ignition, § calculated H_2O. n.d.: not detected. Compositions are quoted in wt.% oxides. 1, 7–10: collinsite from mineralized fissures in serpentinized cataclastic rocks (Fig. 1c): 7–8 a zoned spherulite, 9–10 an aggregate: 9 core, and 10 outermost zone 40 μm in width; 2–7 collinsite from vugs in altered dolomite veins. All data were obtained in this investigation.

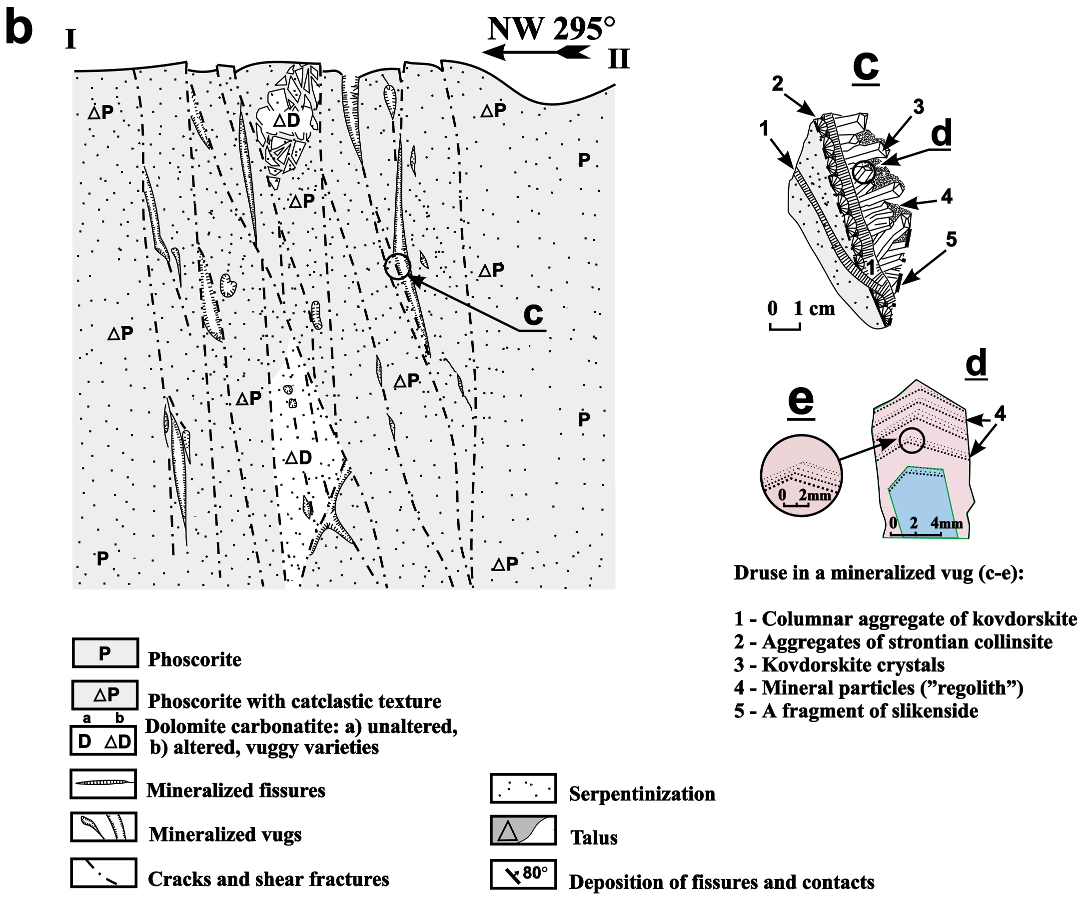

CHEMICAL COMPOSITION

The compositional range of the Kovdor collinsite was determined from 51 quantitative WDS analyses; representative results are shown in Table 1. The initial data show that Sr may be an important constituent of collinsite at Kovdor. The possible presence of tiny Sr-rich impurity phases was ruled out by examining of all the analyzed areas in reflected light and by SEM. In the case of strontiowhitlockite–collinsite aggregates (Fig. 1c), only strontiowhitlockite-free areas of collinsite larger than 100 μm in size were analyzed. To test the analytical data for Sr, collinsite from Reaphook Hill (Australia), Rapid Creek (Yukon Territory) and messelite from Messel (Germany) were analyzed using the same analytical procedure. No Sr was detected in these reference samples.

Most of samples of collinsite analyzed from Kovdor contain from 0.25 to 20.9 wt.% SrO [from 0.01 to 0.74 Sr atoms per formula unit (*apfu*); ΣR^{2+} cations = 3 *apfu*], and some samples contain up to 3.27 wt.% BaO (0.07 *apfu* Ba). There is no correlation between Sr and Ba contents. As illustrated in Figure 3a, the Sr + Ba value is inversely proportional to Ca [correlation coefficient $R = -0.99$, $n = 53$, including the data of Rimskaya-Korsakova (1965) and Kapustin 1980], indicating homovalent substitutions involving Sr and Ba for Ca at the *A* site. The maximum amount of Sr observed in our samples (0.74 *apfu*, see Table 1, anal. 9) corresponds to 37% occupancy of the *A* site, and probably indicates a limit of Sr-for-Ca substitution in the structure of collinsite.

The extent of substitution of Fe and Mn for Mg is negligible in most of the Kovdor samples (Fig. 3b). Only in a very late association with chamosite and bariĉite is collinsite enriched in Fe (0.27–0.31 *apfu* Fe, anal. 2 in Table 1) and depleted in Sr.

X-ray mapping of collinsite from Kovdor (Fig. 4) reveals: i) compositionally homogeneous crystals and aggregates (both Sr-poor and Sr-rich), and ii) aggregates composed of concentric zones of differing Sr:Ca ratio, varying significantly in width (zones thinner than 35–

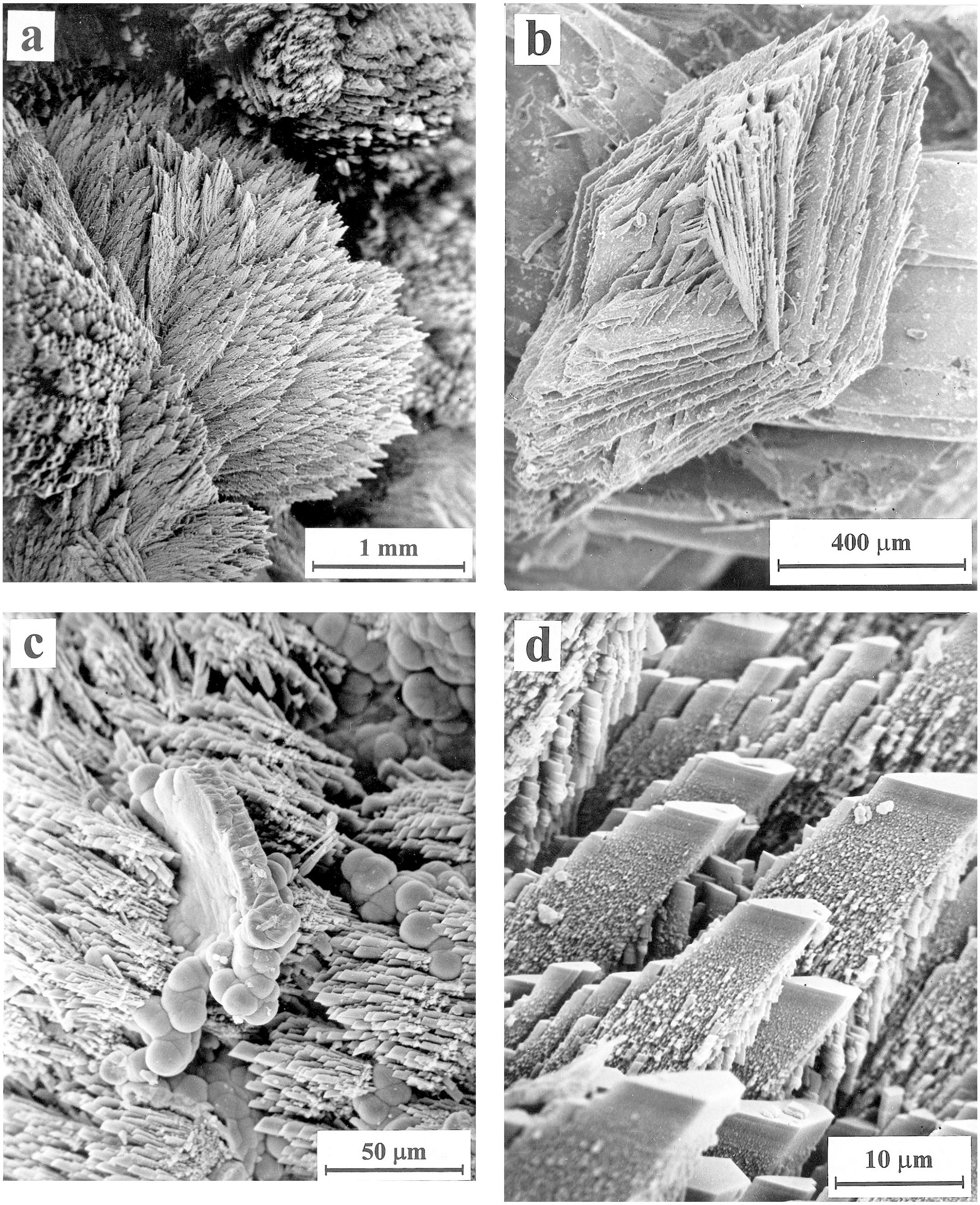

FIG. 2. Morphology of collinsite in vugs of the veins of altered dolomite carbonatite in the NE-trending fault zone. Backscattered electron images. (a) Serrate aggregate of collinsite crystals. (b) Cluster of collinsite crystals on late dolomite. (c) Aggregate of strontiowhitlockite and strontian collinsite. (d) Lamellae of an unidentified late phosphate epitactically overgrowing crystals of collinsite.

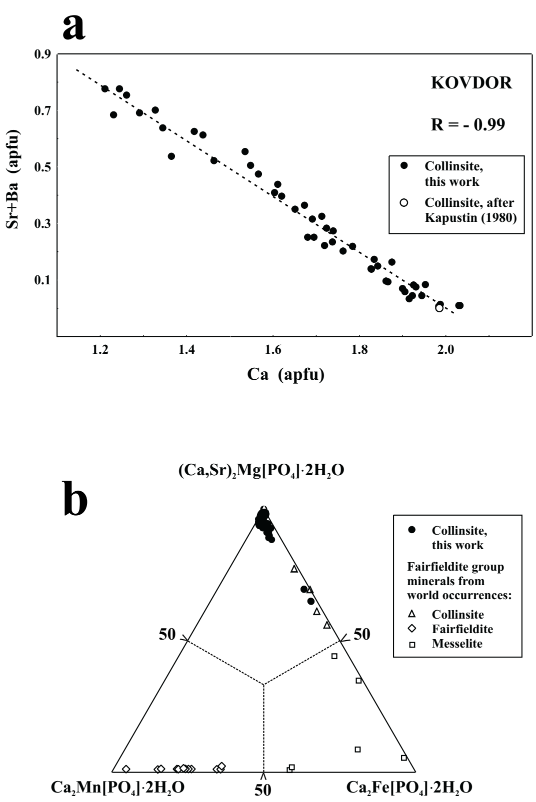

FIG. 3. (a) Concentration of Sr + Ba *versus* Ca *apfu* (atoms per formula unit; ΣR^{2+} cations = 3 *apfu*) in collinsite from Kovdor. Results of 53 analyses (51 original) are plotted. (b) Composition (mol.%) of terrestrial fairfieldite-group minerals. Results of 78 analyses are plotted. Data from Palache *et al.* (1951), Frondel (1955), Rimskaya-Korsakova (1965), and Kapustin (1980) are shown.

40 µm were not analyzed because of the beam diameter employed).

No evidence was found for alteration of collinsite, as Kapustin (1980) had described. We made the suggestion earlier that tiny crystals of messelite may be present on the surface of the collinsite (Liferovich *et al.* 2000a), but this suggestion also lacks support in the present dataset. The lack-luster samples of collinsite that had seemed to be altered, were observed under the SEM to possess lamellae 0.5–5 µm in length epitactically growing on the third-order pinacoids of the crystals (Fig. 2d). These lamellae are similar in shape to the host crystals of collinsite, and the SEM–EDS analyses, made on natural faces, show the presence of P, Ca and Mg in proportions typical of collinsite. Sr, Ba, Fe and Mn were sought, but not detected. Unfortunately, the lamellae are too small for accurate identification.

X-RAY-DIFFRACTION STUDY

X-ray powder-diffraction patterns were obtained for four generations of collinsite with gradually increasing Sr concentrations. Only samples with a variation of ≤0.5–1.0 wt.% in SrO were studied.

All the powder X-ray-diffraction patterns come close to that reported by Kapustin (1980) and deviate from the ASTM–JCPDS standards 26–1063 and 70–1785 in terms of the intensities of the characteristic reflections (Table 2). The unit-cell parameters are compared in Table 3. A systematic increase of *a* and *b* accompanies enrichment in Sr, whereas *c* changes insignificantly. This is in line with details of the crystal structure of collinsite. It is composed of infinite $[Mg(PO_4)_2(H_2O)_2]$ chains parallel to *c*, and the Ca atoms are located in interstices (Hawthorne 1999). Given the significant difference in ionic radius between Ca and Sr (Shannon 1976), one would expect a distortion of the structure in response to incorporation of Sr^{2+}, but the XRD patterns do not exhibit superlattice reflections that could indicate cation ordering or geometrical distortion of the structure. A crystallographic study of strontian collinsite by the Rietveld method is in progress.

INFRARED SPECTROSCOPY

The IR spectra obtained for the strontian and Sr-poor collinsite varieties (Table 1, anal. 1 and 9, respectively) contain similar sets of absorption bands (Fig. 5), those observed for ordinary collinsite (strong bands italicized) being at *3050*, 1646, *1525*, *1105*, *1005*, 942, *768*, *585*, *558* and 448 cm^{-1}, and those for strontian collinsite at *3070*, 1630, *1510*, *1109*, *994*, 941, *746*, *576*, *555*, and 458 cm^{-1}. The IR spectrum for messelite, obtained for comparative purposes, is close to that of strontian collinsite.

The main absorption bands in the collinsite spectra are assigned to the vibrational modes of PO_4 groups and hydrogen-bonded systems. Strong absorption bands at 3050–3070 cm^{-1} and 1510–1525 cm^{-1} indicate that the H_2O molecules form very strong hydrogen bonds with anionic groups, which agrees with the fairly high temperature of dehydration of collinsite (Liferovich *et al.* 2000a). There is some evidence for the higher polarization of H_2O molecules by Ca than by Sr, as the H-bond appears to be stronger in ordinary collinsite than in the strontian variety (3050 cm^{-1} as compared with 3070 cm^{-1}). On the whole, a shift and distortion of some bands are observed in the spectrum for the strontian collinsite, and the shift in the band corresponding to the librational vibrations of H_2O is the most essential difference between the IR spectra of this and the Sr-poor variety. This is due to the difference in the strength of the Ca–H_2O and Sr–H_2O bonds (wavenumbers 768 and 746 cm^{-1}, respectively, Fig. 5).

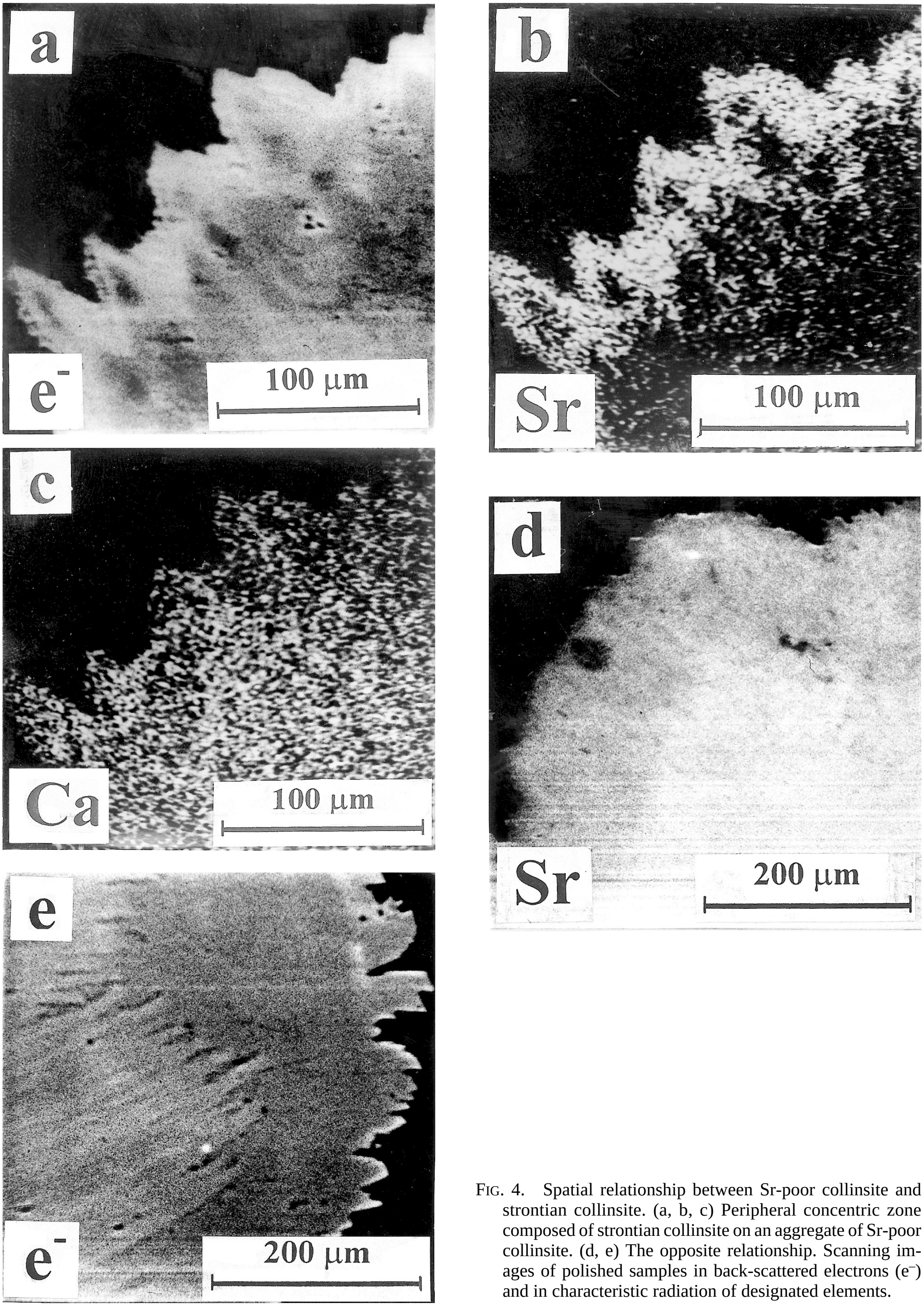

FIG. 4. Spatial relationship between Sr-poor collinsite and strontian collinsite. (a, b, c) Peripheral concentric zone composed of strontian collinsite on an aggregate of Sr-poor collinsite. (d, e) The opposite relationship. Scanning images of polished samples in back-scattered electrons (e^-) and in characteristic radiation of designated elements.

TABLE 2. X-RAY POWDER-DIFFRACTION DATA FOR COLLINSITE

	ASTM JCPDS			Kovdor											
Sr, apfu	0*			0.01**			0.12†			0.23‡			0.74§		
hkl	I_{obs}	d_{obs}	d_{calc}	I_{obs}	d_{obs}	d_{calc}	I_{obs}	d_{obs}	d_{calc}	I_{obs}	d_{obs}	d_{calc}	I_{obs}	d_{obs}	d_{calc}
010	2	6.29	6.277	34	6.31	6.264	9	6.27	6.274	11	6.28	6.275	6	6.33	6.284
100	1	5.10	5.074			5.068	7	5.08	5.076	15	5.10	5.086	5	5.14	5.138
001	4	5.00	5.001	26	5.02	5.016	14	5.01	5.000	17	5.01	5.001	6	5.03	5.017
$\bar{1}01$	3	4.52	4.508	27	4.497	4.497	26	4.51	4.516	43	4.52	4.526	17	4.55	4.569
$\bar{1}11$	<1	3.86	3.845			3.820			3.847			3.851			3.869
011	2	3.52	3.515	35	3.52	3.513			3.514	14	3.52	3.514	3	3.52	3.513
$\bar{1}\bar{1}1$	2	3.51	3.502	10	3.49	3.506	13	3.51	3.508			3.513			3.544
$\bar{1}20$	5	3.24	3.239	65	3.22	3.221	15	3.24	3.235	11	3.24	3.238	10	3.26	3.256
020	5	3.14	3.139	79	3.14	3.132	53	3.14	3.137	41	3.14	3.138	27	3.16	3.142
101	10	3.04	3.037	96	3.04	3.045	37	3.04	3.034	22	3.04	3.036	17	3.07	3.053
$0\bar{2}1$	5	3.02	3.011	75	3.02	3.015			3.009	14	3.02	3.012	8	3.03	3.029
$\bar{2}11$	1	2.757	2.752			2.735			2.754			2.761			2.792
$1\bar{2}1$	6	2.735	2.735			2.734			2.730			2.733			2.755
$\bar{2}10$	8	2.713	2.715	100	2.702	2.705	100	2.713	2.713	100	2.718	2.720	100	2.747	2.752
$\bar{1}21$	3	2.707	2.704			2.702			2.702			2.703			2.708
$\bar{1}02$	9	2.682	2.677	56	2.667	2.678	25	2.681	2.680	41	2.686	2.683	30	2.695	2.698
$0\bar{1}2$	1	2.550	2.547	33	2.550	2.558	15	2.544	2.546			2.548			2.563
200	4	2.540	2.537			2.534			2.538	7	2.543	2.543	9	2.565	2.569
$\bar{1}\bar{2}1$	2	2.468	2.465	18	2.472	2.467	5	2.468	2.467	4	2.471	2.470	5	2.491	2.485
021	2	2.405	2.401			2.402	2	2.403	2.402	3	2.404	2.403			2.409
$\bar{2}21$	3	2.370	2.366			2.346	6	2.367	2.365	7	2.370	2.369	7	2.392	2.387
$\bar{2}\bar{1}1$	4	2.289	2.288	25	2.285	2.287	21	2.290	2.292	12	2.295	2.297	9	2.315	2.319
$0\bar{2}\bar{2}$	4	2.241	2.241			2.250	12	2.238	2.240	8	2.243	2.242	6	2.254	2.258
$\bar{2}12$	3	2.192	2.191			2.180	8	2.193	2.194	13	2.197	2.197	6	2.214	2.214
012	1	2.153	2.149	6	2.156	2.151			2.150			2.148	2	2.156	2.151
$2\bar{1}1$	2	2.137	2.135			2.137			2.133			2.136	6	2.138	2.156
$0\bar{3}1$	1	2.127	2.124			2.124			2.123	7	2.129	2.124			2.134
$\bar{1}\bar{2}2$	4	2.115	2.114	13	2.120	2.121	9	2.118	2.116	10	2.119	2.119			2.135
030	3	2.090	2.092	28	2.090	2.088	8	2.090	2.092	2	2.090	2.092	7	2.090	2.095
$2\bar{2}1$	2	2.061	2.064	10	2.060	2.062	12	2.060	2.060	16	2.064	2.064			2.084
$\bar{2}30$	2	2.006	2.006	20	1.993	1.994	2	2.006	2.003			2.006			2.021
$1\bar{2}\bar{2}$	3	1.993	1.992			1.998	3	1.995	1.989	2	1.993	1.991			2.005
201	2	1.982	1.982			1.985			1.981			1.983	3	1.989	1.997
102	3	1.969	1.969	26	1.979	1.975	7	1.970	1.967	6	1.973	1.968			1.976
$\bar{2}\bar{2}2$	<1	1.923	1.923			1.910			1.923			1.926			1.934
$\bar{3}11$	<1	1.909	1.910			1.900	3	1.912	1.912			1.917	3	1.943	1.943
121	4	1.871	1.871			1.870	7	1.872	1.869	4	1.876	1.869			1.872
$\bar{2}\bar{2}1$	3	1.837	1.836	28	1.832	1.837	11	1.836	1.839	10	1.838	1.841	9	1.860	1.855
$\bar{3}21$	3	1.831	1.831			1.818			1.831			1.836			1.856
$2\bar{3}1$	2	1.821	1.823			1.818			1.819			1.822			1.838
$\bar{3}10$	1	1.804	1.804			1.799	3	1.795	1.803			1.808			1.829
$\bar{1}03$	1	1.796	1.797	26	1.783	1.799	4	1.782	1.798	2	1.799	1.799	7	1.802	1.807
$\bar{3}20$	2	1.778	1.779	28	1.769	1.771	5	1.778	1.778	3	1.784	1.782	5	1.774	1.803
$\bar{3}12$	1	1.766	1.766			1.756			1.768	9	1.769	1.772			1.791
022	3	1.759	1.758			1.756	7	1.760	1.757	2	1.755	1.755			1.756
$1\bar{3}2$	1	1.753	1.753			1.756	6	1.752	1.751			1.753	9	1.720	1.765
$\bar{3}02$	1	1.738	1.736			1.730	3	1.735	1.739	2	1.743	1.744			1.764
220	3	1.698	1.698	25	1.698	1.698			1.699	7	1.699	1.700			1.708
300	4	1.692	1.691			1.689	12	1.691	1.692			1.695			1.713
$\bar{1}13$	4	1.669	1.668	42	1.671	1.668	13	1.662	1.669	12	1.671	1.669	8	1.679	1.673
$\bar{2}13$	3	1.650	1.656	26	1.654	1.652			1.658			1.660			1.668
$0\bar{2}3$	4	1.643	1.648			1.656			1.648	2	1.645	1.650	6	1.659	1.660
$\bar{3}31$	2	1.638	1.637	13	1.621	1.624	3	1.635	1.636			1.639			1.654
$\bar{3}30$	1	1.632	1.633			1.623			1.631			1.634			1.650
$2\bar{2}2$	2	1.617	1.616			1.620			1.614			1.616	1	1.629	1.629
$\bar{1}32$	1	1.593	1.594			1.587	2	1.595	1.593			1.593	2	1.589	1.593
040	1	1.573	1.569	15	1.563	1.566	1	1.570	1.569	3	1.574	1.569			1.571
$3\bar{2}1$	2	1.556	1.555	15	1.555	1.553			1.553			1.556	3	1.550	1.572
$\bar{2}41$	3	1.536	1.535	19	1.535	1.542	2	1.535	1.544	2	1.537	1.535			1.540
$2\bar{3}2$	1	1.519	1.519			1.521	2	1.518	1.516			1.518	4	1.524	1.531
$\bar{2}23$	2	1.504	1.504			1.497	2	1.505	1.504	6	1.508	1.505			1.510

DRON–2.0 diffractometer, graphite-monochromatized Cu*K*α radiation.

*ASTM JCPDS #26–1063, ** corresponds to anal. 2 in Table 1, † corresponds to anal. 3, ‡ corresponds to anal. 5, and § corresponds to anal. 9. Values of d_{obs} and d_{calc} are expressed in Å.

The similarity in IR-spectra between the Sr-poor collinsite, strontian collinsite and messelite may be regarded as indirect evidence in favor of the structural stability of strontian collinsite. Any distortion in the collinsite structure would result in significant differences in the IR spectra, as seen in dimorphous pairs of minerals belonging to the roselite and fairfieldite groups. IR spectra of roselite and wendwilsonite are, for instance, quite different from those of their triclinic counterparts owing to splitting in the region of the stretching and bending modes of the anion group (Pekov *et al.* 2001). The IR spectra obtained in this work do not show any evidence of structural distortion that could be caused by the incorporation of Sr.

STRONTIUM ISOTOPE COMPOSITION

$^{87}Sr/^{86}Sr$ values were obtained for the late phosphates in the collinsite-bearing assemblages. The following were analyzed: i) the coeval strontian collinsite and hydroxylapatite in the mineralized fissures of the serpentine–magnetite cataclasites (N-trending fault), ii) hydroxylapatite, goyazite and crandallite associated with collinsite in a vuggy vein of altered dolomite carbonatite (NE-trending fault), and iii) fresh primary fluorapatite in the less-altered intermediate zone of the same vein. The measured $^{87}Sr/^{86}Sr$ values can be considered initial because of the negligible Rb/Sr values in the phosphates (all Rb contents are ≤3 ppm). The $(^{87}Sr/^{86}Sr)_i$ values obtained range from 0.70330(13) to 0.70380(14) in the late phosphates in the hydrothermal assemblages. With allowances made for the precision of the $^{87}Sr/^{86}Sr$ measurements, both the collinsite and the associated hydrothermal phosphates seem to have formed from solutions with $(^{87}Sr/^{86}Sr)_i$ between 0.70328 and 0.70417. This range overlaps the range of $(^{87}Sr/^{86}Sr)_i$ values of the magmatic phoscorite–carbonatite series at Kovdor given by Zaitsev & Bell (1995) and Verhulst *et al.* (2000), but is much lower than the $(^{87}Sr/^{86}Sr)_i$ values characteristic of the crustal environment (*e.g.*, Archean gneisses around the Kovdor massif and groundwaters that percolate through the gneisses). The $(^{87}Sr/^{86}Sr)_i$ values of the hydrothermal collinsite-bearing assemblages also differ from those of the vuggy dolomite carbonatite that enclose them in the NE-trend-

TABLE 3. UNIT-CELL PARAMETERS OF COLLINSITE

Sr, *apfu*	0*	0.01**	0.12†	0.23‡	0.74§
a Å	5.734	5.704(6)	5.738(9)	5.753(9)	5.824(1)
b Å	6.780	6.761(6)	6.772(8)	6.775(8)	6.800(1)
c Å	5.441	5.454(5)	5.444(5)	5.450(6)	5.479(6)
α °	97.29	97.8(2)	97.3(2)	97.3(2)	97.6(2)
β °	108.56	108.2(2)	108.7(2)	108.8(2)	108.9(2)
γ °	107.28	106.9(1)	107.2(2)	107.2(2)	107.3(3)
V Å^3	185.66	185.15(8)	185.57(6)	186.20(6)	189.62(5)

*ASTM JCPDS #26–1063, ** corresponds to anal. 2 in Table 1, † corresponds to anal. 3, ‡ corresponds to anal. 5, and § corresponds to anal. 9.

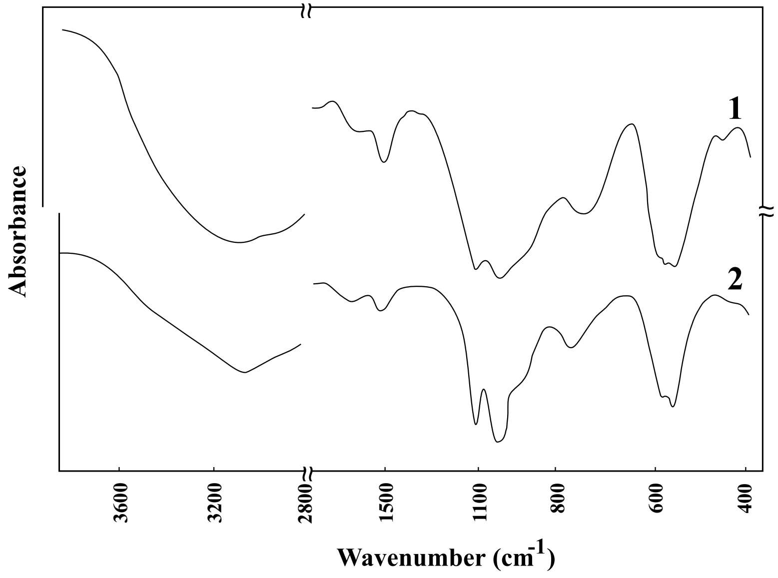

FIG. 5. IR absorption powder spectra of strontian collinsite (1) and Sr-poor collinsite (2), corresponding to anal. 1 and anal. 9 in Table 1.

ing fault. The primary fluorapatite typical of this carbonatite is characterized by $(^{87}Sr/^{86}Sr)_i$ = 0.70510(14), which is in accordance with the data of Landa *et al.* (1982) for a whole-rock dolomite carbonatite, and which differs from the range typical of the massive (unaltered) dolomite carbonatite of the Kovdor massif (Zaitsev & Bell 1995, Verhulst *et al.* 2000). A comparison of $(^{87}Sr/^{86}Sr)_i$ values for the hydrothermal collinsite-bearing assemblages, the vuggy dolomite veins enclosing them, unaltered Kovdor phoscorites and carbonatites, and the Archaean gneisses around the massif is given in Table 4.

Discussion and Conclusions

Sr in collinsite

Our examination of the collinsite-bearing parageneses deposited from the most Sr-rich solutions confirms the assumption made above regarding the limits of Sr incorporation in collinsite. The aggregates that crystallized from such solutions are composed of strontiowhitlockite and collinsite (Fig. 1c), the latter containing 0.23 *apfu* Sr (Table 1, anal. 4), *i.e.*, involving Sr at 11.5% of its *A* site, by comparison with 37% (0.74 *apfu* Sr; Table 1, anal. 9) in the most strontian collinsite. The strontiowhitlockite forms 40–45 vol.% of these aggregates (Fig. 1c; Liferovich *et al.* 2000a) and contains 51.4 wt.% SrO, whereas the residual collinsite contains 6.3–6.9 wt.% SrO (Britvin *et al.* 1991; Table 1, anal. 4). A simple calculation shows that the collinsite–strontiowhitlockite aggregates contain 1.2–1.3 times more Sr than the most markedly strontian collinsite of the same volume. Thus it must have been the marked enrichment of solutions in Sr that caused the deposition of Sr mineral(s) *sensu stricto*, but this did not provoke a progressive incorporation of Sr into the collinsite structure above the limit of 37% of *A* site.

TABLE 4. COMPARISON OF THE $(^{87}Sr/^{86}Sr)_i$ OF COLLINSITE-BEARING ASSEMBLAGES ENCLOSING CARBONATITES AND PHOSCORITES AND GNEISSES AROUND THE KOVDOR MASSIF

Association	Mineral analyzed	SrO wt.%	$(^{87}Sr/^{86}Sr)_i$	±2σ
VI	Crandallite	1.32	0.7038	1.4×10^{-4}
	Goyazite	14.76	0.7037	4.7×10^{-4}
	Strontian collinsite	20.87	0.7035	1.8×10^{-4}
	Hydroxylapatite	1.1–6.02	0.7033–0.7036	1.3×10^{-4}
V	Primary fluorapatite	0.59	0.7051	1.4×10^{-4}
	Whole rock*	0.32	0.7047	1×10^{-4}
IV	Whole rock†	0.28–0.32	0.70353–0.70357	8×10^{-5}
	Fluorapatite‡	0.75	0.70363	3×10^{-5}
III	Fluorapatite from carbonatite and phoscorite‡	0.47–0.75	0.70350–0.70363	3×10^{-5}
II	Fluorapatite from carbonatite and phoscorite‡	0.21–0.30	0.70330–0.70349	3×10^{-5}
I	Archean biotite gneisses of the Belomorian Group§		0.7097–0.7963	1×10^{-4}

$(^{87}Sr/^{86}Sr)_i$ is the initial $^{87}Sr/^{86}Sr$ value (calculated for the Kovdor samples at 380 Ma). Mineral associations: I host rock, igneous phoscorite–carbonatite series, II early calcite series, III late calcite series, IV dolomite carbonatite, V altered vuggy dolomite veins, VI hydrothermal collinsite-bearing assemblages.
References cited: * Landa *et al.* (1982), † Verhulst *et al.* (2000), ‡ Zaitsev & Bell (1995), and § Gorokhov *et al.* (1981).

An explanation for the incorporation of Sr into collinsite could be formulated in terms of bond-valence theory. Brotherton *et al.* (1974) and Hawthorne (1999) have shown a chain of composition $[Mg(PO_4)_2(H_2O)_2]$ to be the main structural unit. This chain possesses a Lewis basicity of 0.25 *v.u.* (valence units), whereas Ca and Sr are characterized by Lewis acidity values of 0.28 *v.u.* and 0.20 *v.u.*, respectively (Hawthorne 1999). In the case of Sr randomly substituting for 37% of Ca at the *A* site, the resulting Lewis acidity of the interstitial cation becomes 0.25 *v.u.* $[(63 \times 0.28 + 37 \times 0.20) / 100]$. As this value satisfies the valence-matching principle, a stable strontian collinsite variety with a disordered arrangement of Sr *versus* Ca forms where Sr is present in the collinsite-forming solutions. Ba is found in collinsite only in minor quantities (Table 1). In addition to the significant difference in ionic radii between Ca^{2+} and Ba^{2+}, the limited incorporation of Ba in the structure may be due to its much lower Lewis acidity relative to that of Ca (Brown 1981). Consequently, Ba accumulated in residual solutions during the crystallization of collinsite and was deposited as rimkorolgite (Britvin *et al.* 1995) or gorceixite (Liferovich *et al.* 1999).

Conditions of the formation of collinsite-bearing assemblages

The conditions under which the hydrothermal processes took place were estimated on the basis of our study of the collinsite-bearing parageneses. The variety of hydrothermal minerals replacing primary pyrrhotite (gladiusite, vivianite, several generations of pyrite, magnetite and pyrrhotite, *etc.*) testifies to the variability of $f(S_2)$, $f(O_2)$ and *pH–Eh* due to the openness of the hydrothermal system, *i.e.*, the lack of equilibrium (Liferovich *et al.* 2000b). The $f(CO_2)$ in hydrothermal solutions was insufficient to form siderite after pyrrhotite, which is a typical product of similar hydrothermal alteration in a carbonatite at Khibina (Zaitsev *et al.* 1998). This relatively low $f(CO_2)$ allowed the upper limit for the temperature of the hydrothermal process to set below 270–250°C, which corresponds to the release of gaseous CO_2 from a carbonatite-derived fluid (carbotherm) that initially had dissolved 30–60 mol.% CO_2 (Bowers & Helgeson 1983, and references therein; Bulakh & Ivanikov 1984, Zaitsev *et al.* 1998). This thermal range agrees well both with data presented by Ting *et al.* (1994) concerning the temperature of homogenization of $H_2O–CO_2$ fluid inclusions in carbonatites, and with data given by Pirogov (1987) showing that a postmagmatic generation of apatite in the Kovdor carbonatites has trapped the liquid inclusions which decrepitate at 270°C. Cocrystallization of the hexagonal pyrrhotite and collinsite shows that temperature of their deposition was above 248°C, according to the data of Kissin & Scott (1972) on the crystallization of iron monosulfide polymorphs from aqueous solutions. These estimates agree with range of 270–120°C given by Moore (1973) for the crystallization of fairfieldite-group minerals in highly fractionated pegmatites. We thus suggest that the collinsite-bearing assemblages at Kovdor were formed under similar low-temperature conditions.

The $(^{87}Sr/^{86}Sr)_i$ characteristics of the collinsite-bearing assemblages (Table 4) shed light on the source of the hydrothermal solutions, which must have been derived from an orthomagmatic fluid fractionated from the mantle-derived Kovdor phoscorites and carbonatites, *i.e.*, they were juvenile by definition. The fluid was not derived immediately from the ^{87}Sr-rich veins of dolomite carbonatites that host the hydrothermal assemblages. Without going into details, we can suggest, according to model of Farver & Giletti (1989), that the primary fluorapatite in the unaltered (intermediate) parts of the dolomite veins had been enriched with ^{87}Sr as a result of dynamothermal metamorphism (caused by postmagmatic disturbances along the NE-trending fault) *i.e.*, without any contribution from the crustal component. Whole-rock enrichment of a dolomite carbonatite with ^{87}Sr, as described by Landa *et al.* (1982), probably had more complex reasons and could be due to the redistribution of ^{87}Sr from the Rb-rich jacupirangite (Verhulst *et al.* 2000) that had been cross-cut by the dolomite carbonatite and underwent the same dynamothermal disturbances.

Recent findings by Barrat *et al.* (2000) show the susceptibility of the apatite structure to Sr introduction under metamorphism and the resistance of the structure to removal of the secondary Sr by any solutions, even through partial leaching of the mineral. Creaser & Gray (1992) demonstrated the preservation of the $(^{87}Sr/^{86}Sr)_i$ ratio in apatite upon the hydrothermal alteration of an igneous rock. This leads us to formulate at least three conclusions: i) the relatively high $^{87}Sr/^{86}Sr$ value in the primary fluorapatite of the dolomite carbonatite had not been changed *via* hydrothermal alteration of the carbonatite, and can thus provide correct information on the dynamothermal event that took place before these alterations; ii) the hydrothermal hydroxylapatite in the mineralized vugs could not have been depleted in ^{87}Sr as a result of any epigenetic waters that entered the hydrothermal system (an influx of the groundwater into the system has been taking place for at least the last 35 years, during which time phoscorites and carbonatites have been intensively mined in an inundated open pit); iii) the similarity in Sr isotope compositions of the collinsite, goyazite and crandallite, which are coeval with the hydroxylapatite (Table 4), demonstrates the preservation of $(^{87}Sr/^{86}Sr)_i$ values in these species as well.

Unfortunately, examination of the stable isotope systems in the same hydrothermal minerals may provide misleading data on account of the unknown behavior of these systems in complex hydroxy-hydrated phosphates in contact with epigenetic solutions; the ε_{Nd} *versus* ε_{Sr} approach to the genetic consideration is hampered by lack of *REE* in the hydrothermal phosphates of the Kovdor complex (Liferovich *et al.* 1999).

We can assume from the textural evidence and the Sr isotope characteristics that collinsite-bearing assemblages were superimposed upon the dolomite carbonatite veins, and thus, the mineralized veins of vuggy dolomite carbonatite should not be regarded as a peculiar, highly fractionated carbonatite, enriched in the volatiles, P, Sr, and Ba. Although the hydrothermal collinsite-bearing assemblages sampled here are confined to faults relatively near the surface, groundwater did not contribute crustal Sr to the hydrothermal system. This feature can be explained in terms of an upward flow of juvenile solutions under high pressure that did not allow for marked influx of crustal water prior to the crystallization of the hydrothermal phosphates.

The deposition of assemblages from hydrothermal solutions that differed markedly from their host rocks in $(^{87}Sr/^{86}Sr)_i$ shows that these assemblages were formed under conditions that were unfavorable for the homogenization of $^{87}Sr/^{86}Sr$ values between the rock and the fluid through intense rock–fluid interaction. Homogenization of the Sr isotope composition between the carbonate rock and the hydrous solutions was not achieved within the temperature range 270–110°C under conditions of wide variations in pH–Eh, $f(O_2)$, $f(S_2)$ and relatively low $f(CO_2)$.

The history of growth of the collinsite-bearing assemblages clearly indicates the complicated nature of the hydrothermal processes that take place in carbonatites associated with alkaline-ultramafic massifs. It illustrates the final stage in the crustal evolution of mantle-derived orthomagmatic fluids.

ACKNOWLEDGEMENTS

This study was supported by the Academy of Finland, CIMO foundation (RPL) and INTAS (RPL and YAP). We are grateful to the referees, Anton R. Chakhmouradian and Yuanming Pan, to Associate Editor Roger H. Mitchell, and to Robert F. Martin for helpful reviews and criticism. We thank Mr. Tim Jokela, Mr. Dermot Henry (Museum of Natural Sciences of Australia), Dr. Steffen Möckel (Germany), Mr. Sergei Britvin and Dr. Grigory Ivanyuk, who provided samples for comparison. We are grateful to Mr. Malcolm Hicks for improving the English of the manuscript. We thank the management staff of the “AO Kovdorsky GOK” and geologists Alexandr Bykhovets, Eugeny Krasovsky and

Alexandr Putilov, for their valuable help during the fieldwork. The authors are grateful to Mr. Alexei Delenitsin, Drs. Dmitry Makarov and Oleg Zalkind at the Kola Science Centre, Russian Academy, and Mr. Olli Taikina-aho, Raja Peura, and Elvi Hiltola at the Institute of Electron Optics, University of Oulu, for their assistance.

References

Barrat, J.A., Taylor, R.N., André, J.P., Nesbitt, R.W. & Lecuyer, C. (2000): Strontium isotopes in biogenic phosphates from a Neogene marine formation: implications for palaeoseawater studies. *Chem. Geol.* **168**, 325-332.

Bayanova, T.B., Kirnarsky, Yu.M. & Levkovich, N.V. (1997): U–Pb dating of baddeleyite from rocks of the Kovdor massif. *Dokl. Acad. Nauk USSR, Earth Sci. Sect.* **356**, 1094-1096.

Bowers, T.S. & Helgeson, H.C. (1983): Calculation of the thermodynamic and geochemical consequences of nonideal mixing in the system H_2O–CO_2–NaCl on phase relations in geologic systems: equation of state for H_2O-CO_2-NaCl fluids at high pressures and temperatures. *Geochim. Cosmochim. Acta* **47**, 1247-1275.

Bridge, P.J. & Pryce, M.W. (1974): Magnesian collinsite from Milgun Station, Western Australia. *Mineral. Mag.* **39**, 577-579.

Britvin, S.N., Pakhomovskii, Ya.A., Bogdanova, A.N., Khomyakov, A.P. & Krasnova, N.I. (1995): Rimkorolgite, $(Mg,Mn)_5(Ba,Sr,Ca)(PO_4)_4{\bullet}8H_2O$, a new mineral from the Kovdor iron deposit, Kola Peninsula. *Zap. Vser. Mineral. Obshchest.* **124**(1), 90-95 (in Russ.).

________, ________, ________ & Skiba, V.I. (1991): Strontiowhitlockite, $Sr_9Mg(PO_3OH)(PO_4)_6$, a new mineral species from the Kovdor deposit, Kola Peninsula, USSR. *Can. Mineral.* **29**, 87-93.

Brotherton, P.D., Maslen, E.N., Pryce, M.W. & White A.H. (1974): Crystal structure of collinsite. *Aust. J. Chem.* **27**, 653-655.

Brown, I.D. (1981): The bond-valence method; an empirical approach to chemical structure and bonding. *In* Structure and Bonding in Crystals **2** (M. O'Keeffe & A. Navrotsky, eds.). Academic Press, New York, N.Y. (1-30).

Bulakh, A.G. & Ivanikov, V.V. (1984): *The Problems of Mineralogy and Petrology of Carbonatites*. Leningrad University Publ., Leningrad, Russia (in Russ.).

Creaser, R.A. & Gray, C.M. (1992): Preserved initial $^{87}Sr/^{86}Sr$ in apatite from altered igneous rocks: a case study from the Middle Proterozoic of South Australia. *Geochim. Cosmochim. Acta* **56**, 2789-2795.

Dunaev, V.A. (1982): Structure of the Kovdor deposit. *Geol. of Ore Deposits* **3**, 28-36 (in Russ.).

Farver, J.R. & Giletti, B.J. (1989): Oxygen and strontium diffusion kinetics in apatite and potential applications to thermal history determinations. *Geochim. Cosmochim. Acta* **53**, 1621-1631.

Frondel, C. (1955): Neomesselite and beta-roselite: two new members of the fairfieldite group. *Am. Mineral.* **40**, 828-833.

Gorokhov, I.M., Kutyavin, E.P., Volodichev, O.I., Duk, V.L., Varshavskaya, E.S. & Krylov, I.N. (1981): Rb–Sr dating of magmatic and metamorphic rocks of Belomorian complex (western Belomorie). *Sov. Geol.* **3**, 67-75 (in Russ.).

Hawthorne, F.C. (1999): Structure and chemistry of phosphate minerals. *Mineral. Mag.* **62**, 141-164.

Kapustin, Yu.L. (1980): *Mineralogy of Carbonatites*. Amerind Publ. Co., New Delhi, India.

Khomyakov, A.P., Alexandrov, V.B., Krasnova, N.I., Ermilov, V.V. & Smol'yaninova, N.N. (1982): Bonshtedtite $Na_3Fe(PO_4)(CO_3)$ – a new mineral. *Zap. Vser. Mineral. Obshchest.* **111**(4), 486-490 (in Russ.).

Kissin, S.A. & Scott, S.D. (1972): Phase relations of intermediate pyrrhotites. *Econ. Geol.* **67**, 1007 (abstr.).

Kogarko, L.N., Kononova, V.A., Orlova, M.P. & Wooley, A.R. (1995): *Alkaline Rocks and Carbonatites of the World.* **2**. *Former USSR*. Chapman and Hall, London, U.K.

Krasnova, N.I. & Kopylova, L.N. (1988): The geological basis ore for the mineralogical–technological mapping at the Kovdor ore deposit. *Int. Geol. Rev.* **30**, 307-319.

Kukharenko, A.A., ed. (1965): *The Caledonian Complex of the Ultramafic, Alkaline Rocks, and Carbonatites of the Kola Peninsula and North Karelia*. Nedra, Moscow, Russia (in Russ.).

Landa, E.A., Murina, G.A., Shergina, Yu.P. & Krasnova, N.I. (1982): Isotopic composition of strontium in apatite and apatite-bearing rocks of carbonatite complexes. *Dokl. Acad. Sci. USSR* **264**, 214-216.

Liferovich, R.P., Pakhomovsky, Ya. A. & Bogdanova, A.N. (2000a): Fairfieldite group minerals form the Kovdor massif. *Zap. Vser. Mineral. Obshchest.* **129**(4), 95-107 (in Russ.).

________, Sokolova, E.V., Hawthorne, F.C., Laajoki, K.V.O., Gehör, S., Pakhomovsky, Ya.A. & Sorokhtina, N.V. (2000b): Gladiusite, $Fe^{3+}_2(Fe^{2+},Mg)_4(PO_4)(OH)_{11}(H_2O)$, a new hydrothermal mineral species from the phoscorite–carbonatite unit, Kovdor Complex, Kola Peninsula, Russia. *Can. Mineral.* **38**, 1477-1485.

________, Yakovenchuk, V.N., Pakhomovsky, Ya.A., Bogdanova, A.N. & Stümpel, G. (1999): Crandallite, goyazite and gorceixite from the Kovdor massif, Russia. *Neues Jahrb. Mineral., Monatsh.*, 145-166.

MOORE, P.B. (1973): Pegmatite phosphates: descriptive mineralogy and crystal chemistry. *Mineral. Rec.* **4**, 103-130.

PALACHE, C., BERMAN, H. & FRONDEL, C. (1951): *The System of Mineralogy.* Harvard University. J. Wiley and Sons, New York, N.Y.

PEKOV, I.V., VINOGRADOVA, R.A., CHUKANOV, N.V. & KULIKOVA, I.M. (2001): On magnesium and cobalt arsenates of fairfieldite and roselite groups. *Zap. Vser. Mineral. Obshchest.* **130** (in press).

PIROGOV, B.I. (1987): *Dependence of Technological Properties of the Kovdor Apatite and Heavy Fraction on the Kovdor Ores Peculiarities*. Sci. Report, Krivorozhsky Gornorudny Inst. (in Russ.).

PONOMAREVA, E.V. & KRASNOVA, N.I. (1990): New data on kovdorskite – $Mg_2(PO_4)(OH)•3H_2O$. *Zap. Vses. Mineral. Obshchest.* **119**(6), 92-100 (in Russ.).

RIMSKAYA-KORSAKOVA, O.M. (1965): Collinsite. *In* The Caledonian Complexes of Alkaline-Ultrabasic and Carbonatite Rocks on Kola Peninsula and in Northern Karelia (A.A. Kukharenko, ed.). Nedra, Moscow, Russia (521-522; in Russ.).

ROBINSON, G.W., VAN VELTHUISEN, J., ANSELL, H.G. & STURMAN, B.D. (1992): Mineralogy of the Rapid Creek and Big Fish River area, Yukon Territory. *Mineral. Rec.* **23**, 1-47.

SHANNON, R.D. (1976): Revised effective ionic radii and systematic studies of interatomic distances in halides and chalcogenides. *Acta Crystallogr.* **A32**, 751-767.

STEIGER, R.N. & JÄGER, E. (1977): Subcomission on geochronology: Convention on the use of decay constants in geo- and cosmochronology. *Earth Planet. Sci. Lett.* **36**, 359-362.

TERNOVOI, V.I. (1977): *Carbonatite Massifs and Their Ores.* Leningrad State University Press, Leningrad, Russia (in Russ.).

TING, W., BURKE, E.A.J., RANKIN, A.H. & WOOLLEY, A.R. (1994): Characterisation and petrogenetic significance of CO_2, H_2O and CH_4 fluid inclusions in apatite from the Sukulu carbonatite, Uganda. *Eur. J. Mineral.* **6**, 787-803.

VERHULST, A., BALAGANSKAYA, E., KIRNARSKY, Y. & DEMAIFFE, D. (2000): Petrological and geochemical (trace elements and Sr/Nd isotopes) characteristics of the Paleozoic Kovdor ultramafic, alkaline and carbonatite intrusion (Kola peninsula, NW Russia). *Lithos* **51**, 1-25.

ZAITSEV, A. & BELL, K. (1995): Sr and Nd isotope data of apatite, calcite and dolomite as indicators of the source, and the relationships of phoscorites and carbonatites from the Kovdor massif, Kola peninsula, Russia. *Contrib. Mineral. Petrol.* **121**, 324-335.

________, SINAI, YU.M., CHAKHMOURADIAN, A.R. & LEPEKHINA, E.N. (1998): Pyrrhotite – pyrite association in carbonatite series rocks of Khibina alkaline massif. *Zap. Vser. Mineral. Obshchest.* **127**(4), 110-119 (in Russ.).

Received September 21, 2000, revised manuscript accepted July 12, 2001.